

Simultaneous determination of diclofenac and indomethacin using a sensitive electrochemical sensor based on multiwalled carbon nanotube and ionic liquid nanocomposite

Kianoush Sarhangzadeh · Ali Akbar Khatami ·
Mohammad Jabbari · Siavash Bahari

Received: 14 March 2013 / Accepted: 8 August 2013 / Published online: 21 August 2013
© Springer Science+Business Media Dordrecht 2013

Abstract Multiwalled carbon nanotube and ionic liquid-modified carbon ceramic electrode (MWCNT-IL/CCE) was employed for the simultaneous determination of diclofenac and indomethacin (IND). The measurements were carried out by differential pulse voltammetry method in optimal conditions. The prepared electrode showed appropriate voltammetric responses to DCF and IND with 0.225 V difference in the oxidation peak potentials, making fabricated electrode suitable for simultaneous determination of these compounds. The calibration curves were linear over a wide range of concentrations of each species including 0.05–50 $\mu\text{mol L}^{-1}$ for DCF and 1–50 $\mu\text{mol L}^{-1}$ for IND. Detection limits were found to be 18 and 260 nM for DCF and IND, respectively. The developed method having good stability and sensitivity was successfully applied for DCF and IND in commercial tablet as well as human blood plasma samples.

Keywords Indomethacin · Diclofenac · Ionic liquid · Carbon nanotube · Modified electrode

1 Introduction

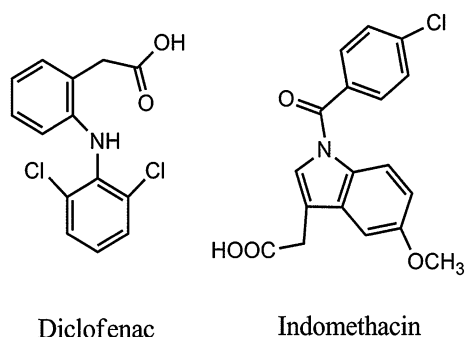
Non-steroidal anti-inflammatory drugs (NSAIDs) are a series of drugs providing antipyretic, analgesic, and anti-inflammatory effects. All compounds in this class act by inhibition of cyclooxygenase enzymes, which are involved in inflammation. They are also responsible for the synthesis

of prostaglandins involved in normal physiological processes. Inhibition of these actions is responsible for the majority of the adverse effects of NSAIDs in clinical use, and for their main toxicity in overdose [1–3]. Indomethacin (IND) and diclofenac (DF) (Scheme 1) are important non-steroidal anti-inflammatory drugs used to treat several pathologies. DF is one of the most common NSAID and extensively used in clinical medicine for the treatment of rheumatoid arthritis, osteoarthritis, non-articular rheumatism, and sport injuries [4, 5]. Also, in NSAID drugs group, IND, is known for its antipyretic and analgesic actions [6]. IND is metabolized in vivo and used in the treatment of some forms of inflammatory and degenerative diseases of articulations, such as osteoarthritis, rheumatoid arthritis, and gout [7–9].

Since carbon nanotubes (CNTs) were discovered [10], due to their unique properties, such as high external surfaces, good electronic conductivity, and high stability, (CNTs) have attracted more and more interest in the applications of the new carbon materials in a variety of fields, including chemical and biological sensors [11, 12], separation membranes [13, 14], field emission devices [15, 16], energy storage [17], and so on.

Ionic liquids (ILs) are kinds of ionic compounds, which exist in liquid state at room temperature. Because of their unusual properties such as high chemical and thermal stability, negligible vapor pressure, relatively high ionic conductivity, and wide electrochemical windows [18, 19], ILs have received much attention in electrochemistry [20, 21], catalysis [22], organic synthesis [23], and liquid–liquid extraction [24]. Recently, ILs have been used as the paste binders for fabricating carbon composite electrodes, which provide an obvious increase in the electrochemical response of electroactive substrates and reduce the overpotentials of some organic substances [25].

K. Sarhangzadeh (✉) · A. A. Khatami · M. Jabbari · S. Bahari
Department of Chemistry, Ahar Branch, Islamic Azad
University, 5451116714 Ahar, Iran
e-mail: k.sarhangzadeh@yahoo.com



Scheme 1 Chemical structure of DF and IND

Drug analysis has an extensive impact on public health. Electrochemical techniques have been used for the determination of a wide range of drug compounds without derivatization. Compared with other techniques, electrochemical methods are characterized by portability, simplicity, minimal cost, and reasonably short analysis time. To the best of our knowledge, no report based on simultaneous determination of IND and DF by using a MWCNT–IL nanocomposite-modified carbon ceramic electrode (CCE) has been found. This paper describes a simple and fast procedure for the fabrication of CCE modified with MWCNT–IL. Modified CCE was used for determination of DCF and IN in the individual and mixture solution. Finally, the analytical performance of this sensor for simultaneous determinations of these species was evaluated in commercial pharmaceutical and plasma samples by differential pulse voltammetry (DPV) and results indicated that determination of DCF and IN in biological samples could be well proceeded.

2 Experimental

2.1 Chemicals

All the chemicals were used in analytical grade, and all the solutions were prepared in double distilled water. IND and DCF were purchased from Zahravi pharmaceutical Co., Tabriz, Iran. Methyltrimethoxysilane (MTMOS) and powdered graphite were purchased from Merck. CH_3COOH , H_3BO_3 , H_3PO_4 , HCl , and other reagents were from Merck or Aldrich. MWCNT with 95 % purity was obtained from Nanolab (Brighton, MA), and IL and 1-butyl-3-methylimidazolium hexafluorophosphate (BMIMPF_6 , 98 %) were obtained from Sigma (USA). Britton–Robinson buffer (B–R, 0.04 mol L^{-1} , pH 7.0), as supporting electrolyte, was prepared by mixing $0.04 \text{ mol L}^{-1} \text{H}_3\text{BO}_3$, $0.04 \text{ mol L}^{-1} \text{CH}_3\text{COOH}$, and $0.04 \text{ mol L}^{-1} \text{H}_3\text{PO}_4$, and the required pH was adjusted by using $0.5 \text{ mol L}^{-1} \text{NaOH}$.

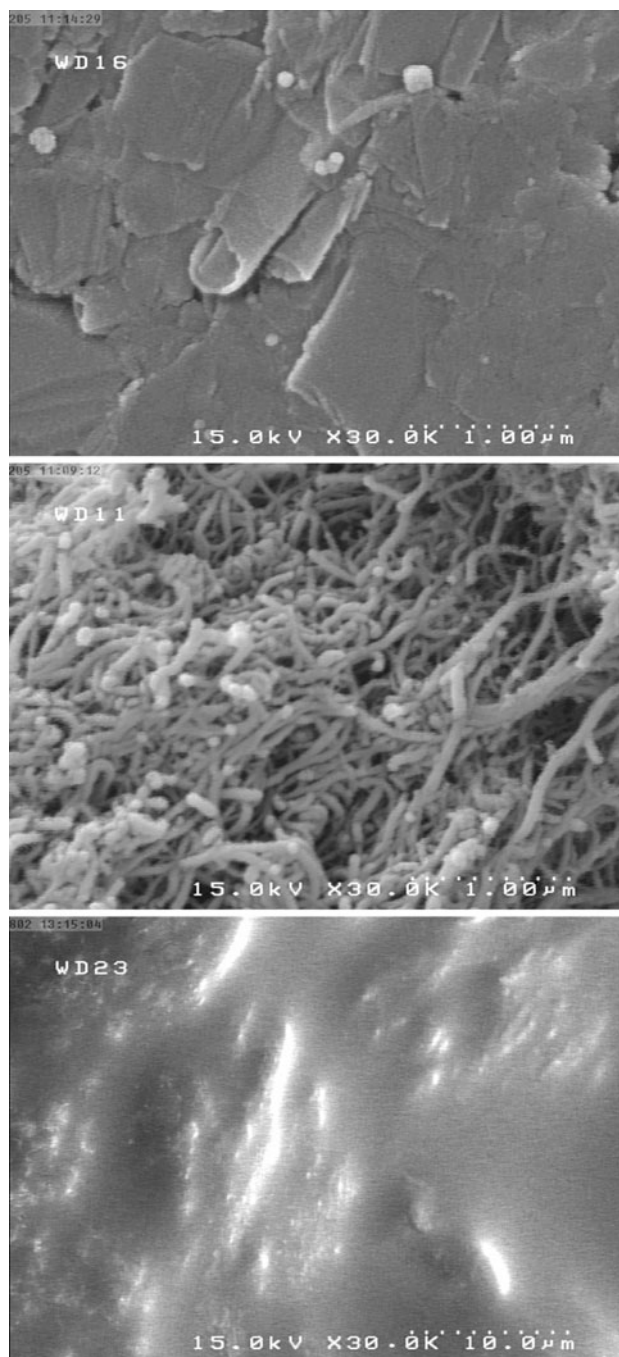


Fig. 1 FESEM images of **a** CCE surface immediately after polishing, **b** MWCNT/CCE, and **c** MWCNT–IL/CCE

2.2 Apparatus

All the electrochemical measurements were performed on an AUTOLAB PGSTAT-100 (potentiostat/galvanostat) in a three-electrode system. The working electrode was a MWCNTs–IL composite film-coated CCE, MWCNTs–IL/CCE, (geometric surface area of 0.119 cm^2). A platinum wire and a saturated calomel electrode (SCE) were used as

the counter and reference electrodes, respectively. The morphology of the films was studied by field emission scanning electron microscopy (Hitachi, model S-4160).

2.3 Preparation of bare carbon ceramic electrode

Due to some unique properties of CCE including high porosity, renewable surface, good conductivity, and economical fabrication, it was used as a substrate for MWCNTs–IL composite. The bare CCE was prepared according to the procedure described by Lev and coworkers [26] by mixing 0.15 mL MTMOS, 0.30 mL methanol, and 10 μL hydrochloric acid (11 M). This mixture was magnetically stirred for 2 min. Then 0.3 g graphite powder was added and the resultant mixture was shaken for another 1 min. A 5-mm-long Teflon tube (3–4 mm inner diameter) was filled with the sol–gel carbon mixture and dried under ambient conditions (25 $^{\circ}\text{C}$).

2.4 Preparation of the MWCNT–IL/CCE

20 μL IL (BMIMPF₆) was mixed with 1 mg mL^{−1} MWCNTs in DMF:water (1:3) solution and the resulted

mixture was sonicated in ultrasonic bath about 30 min to obtain a viscous MWCNTs–IL composite. 20 μL of the obtained composite was dropped on the cleaned CCE surface and dried in room temperature for 24 h. Afterward the MWCNTs–IL/CCE is ready to use.

3 Results and discussions

3.1 Characterization of MWCNT–IL/CCE

FESEM was used to surface characterization of CCE, MWCNTs/CCE, and MWCNTs–IL/CCE and the results are presented in Fig. 1. The surface of the bare CCE immediately after being polished is presented in Fig. 1a. The image depicts that the surface is scaly, porous, and dense. As can be seen on the surface of CCE (Fig. 1b) the MWCNTs were distributed homogeneously on the surface of the electrode with a special three-dimensional structure; When IL is introduced in the MWCNT structure, the film becomes more uniform and even, this is related to the binding and blanketing effect of IL (Fig. 1c).

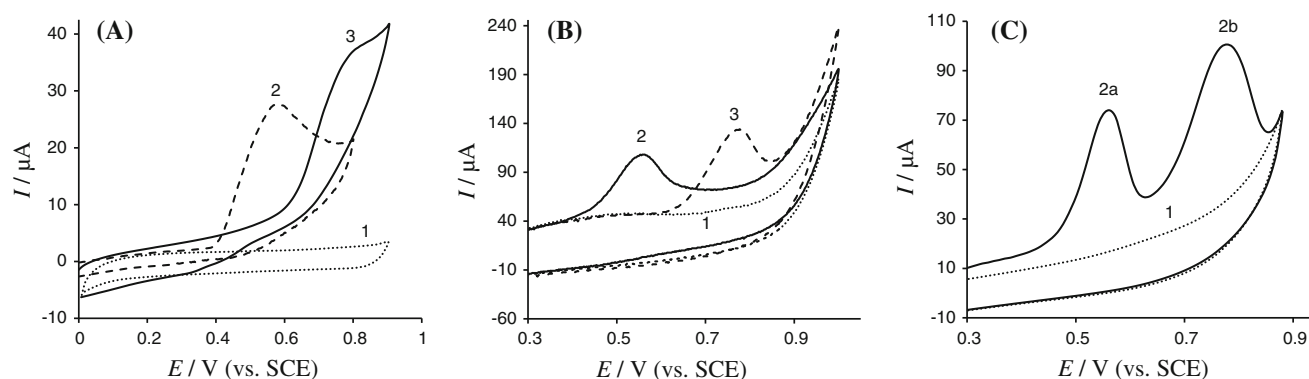
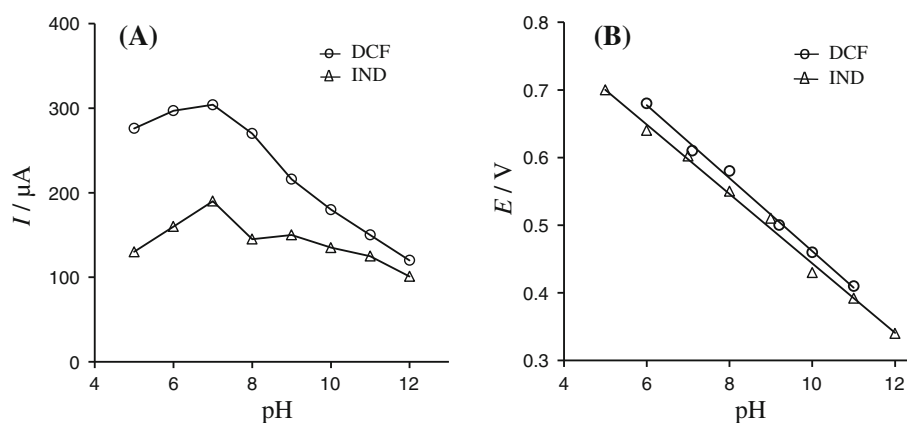


Fig. 2 CVs recorded **a** at the bare CCE in the absence (1) and in the presence of 1.0 mM DCF (2) and 0.5 mM IND (3), **b** at the MWCNT–IL/CCE in the absence (1) and in the presence of 1.0 mM DCF (2) and 0.5 mM IND (3), and **c** at the MWCNT–IL/CCE in the

absence (1) and presence of 1.0 mM DCF + 0.5 mM IND (peak 2a and 2b), respectively, in B–R buffer solution (pH 7.0), Scan rate: 50 mV s^{-1}

Fig. 3 Effect of pH on the peak current (**a**) and on the peak potential (**b**) of 1.0 mM DCF and IND in B–R buffer solution



3.2 Electrocatalytic oxidation of IND and DCF at the surface of MWCNTs–IL/CCE

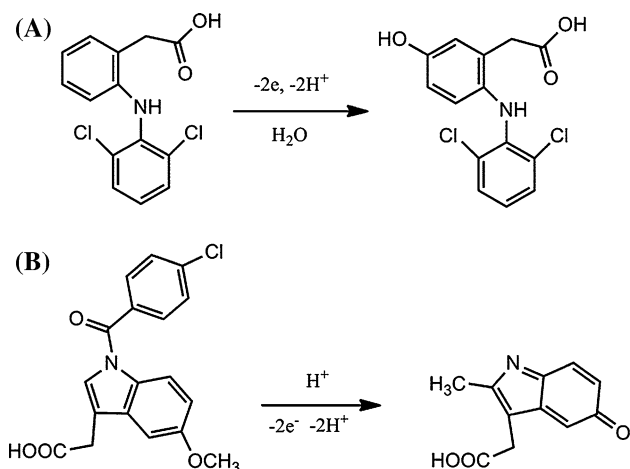
Our primary survey showed that the electrochemical detection of IND in the presence of DCF on untreated ordinary electrodes is difficult due to the oxidation peak of IND at the potential close to DCF that results in an overlapped voltammetric response and low currents. To confirm this, the electrochemical behavior of IND and DCF on the surface of the bare CCE was investigated. Figure 2a depicts cyclic voltammograms (CVs) of the bare CCE in the absence (a) and presence of 1.0 mM DCF (curve b) and 0.5 mM IND (curve c) in B–R buffer solution (pH 7.0). Background curve (a) shows that, the CV of B–R buffer solution at the bare CCE in the potential ranges from 0 to 0.9 V has no oxidation and reduction peaks. On the other hand, DCF shows an oxidative peak at 566 mV, and IND demonstrates oxidation peak at 800 mV. As can be seen on the surface of the electrode, oxidations of DCF and IND are irreversible.

Figure 2b shows the CVs of the IND and DCF on the surface of the MWCNT–IL/CCE. The anodic peak potential of DCF shifts from 566 mV at the bare CCE to 547 mV at the MWCNT–IL/CCE, and the anodic peak current is enhanced approximately two times in comparison with the

anodic peak current on CCE. However, the anodic peak potential for the oxidation of IND occurs at 772 mV, which is ~ 28 mV more negative than its CV at the bare CCE, and the anodic peak current is enhanced approximately five times in comparison with the anodic peak current on the CCE. The decrease of oxidation overpotential, accompanied by a significant increase in the oxidation current of IND and DCF, indicates excellent catalytic ability of MWCNT–IL composite on the oxidation of these compounds.

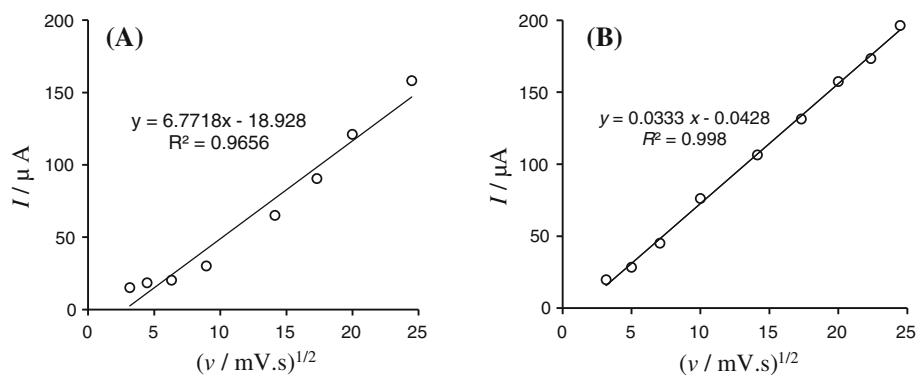
3.3 Electrochemical behavior of DCF and IND in mixture

We also studied the electrochemical behaviors of DCF and IND in the mixture solution. Figure 2c shows the CVs of the mixture solution at the MWCNT–IL/CCE. The obtained voltammetric peaks for DCF and IND at the MWCNT–IL/CCE appear at 563 and 778 mV in B–R buffer solution (pH 7.0). Larger separation of the peak potentials allows them to be simultaneously detected in mixtures. The above-obtained results demonstrate that MWCNT–IL accelerates the oxidation of DCF and IND because of much edge plane graphite and improves the peak separation between DCF and IND dramatically. On the other hand, the remarkable peak current enhancement and the drop of oxidation overpotentials undoubtedly testify the electrocatalytic properties of the MWCNT–IL/CCE in the oxidation of these compounds. Indeed, the MWCNT–IL/CCE presents an interlinked highly mesoporous three-dimensional structure with a relatively higher electrochemically accessible surface area and easier charge transfer at the electrode/electrolyte interface [27]. Also the effective surface area of MWCNT–IL was evaluated by CV using potassium ferricyanide as a probe at various scan rates. According to the Randles–Sevcik equation [28], the effective surface area of the MWCNT–IL was calculated to be 0.36 cm^2 . The same procedure was used for obtaining the effective surface area of CCE which was calculated to be 0.16 cm^2 . The increased effective surface area of MWCNT–IL/CCE in comparison with CCE indicated that



Scheme 2 Oxidation mechanism of DCF (a) and IND (b)

Fig. 4 Plots of I_p versus v for 0.5 mM DCF (a) and I_p versus $v^{1/2}$ for 1.5 mM IND (b) derived from cyclic voltammograms of MWCNTs–IL nanocomposite-modified CCE in B–R buffer solution (pH 7.0), at different scan rates



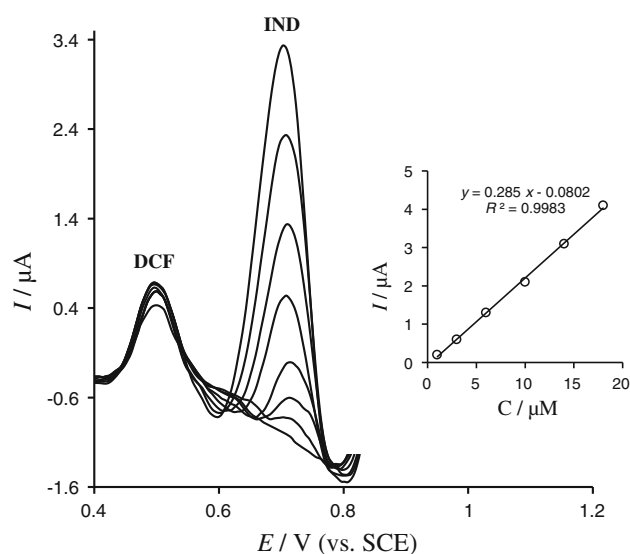


Fig. 5 DPVs of DCF at MWCNT-IL/CCE in the presence of 2 μM IND in B-R buffer (pH 7.0) DCF concentrations (from inner to outer): 0.05, 0.2, 0.4, 1, 2, and 4 μM

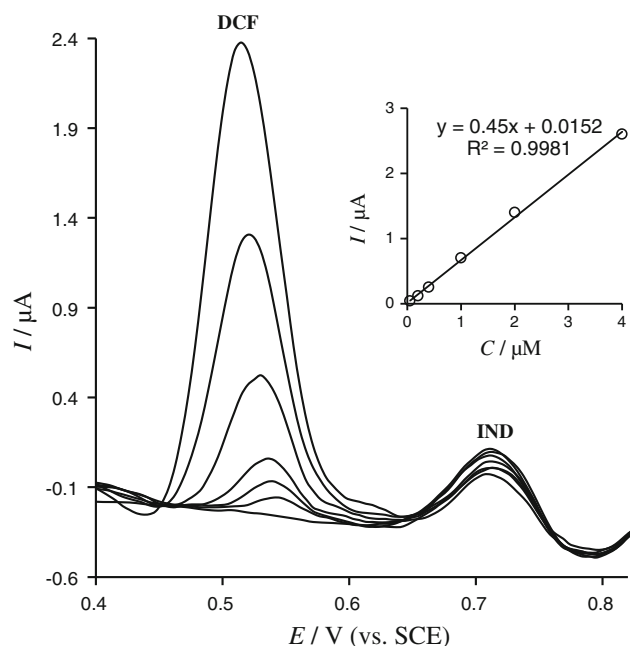


Fig. 6 DPVs of IND at MWCNT-IL/CCE in the presence of 2 μM DCF in B-R buffer (pH 7.0) IND concentrations (from inner to outer): 1, 3, 6, 10, 14, and 18 μM

the MWCNT-IL effectively enhanced the surface area as well as the reactivity of the MWCNT-IL/CCE surface.

3.4 Effect of buffer component and solution pH

The electrochemical responses of IND were studied in different media, namely acetate, phosphate, and B-R buffer solution. The maximal peak currents of IND were obtained

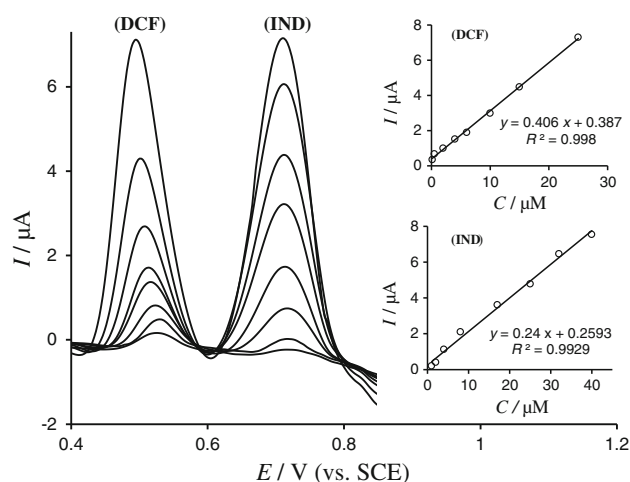


Fig. 7 DPVs of the mixture containing DCF and IND at the MWCNT-IL/CCE in B-R buffer (pH 7.0). Concentrations of the two compounds (from inner to outer): 0.05, 0.2, 0.4, 1, 2, and 4 μM for DCF; and 1, 3, 6, 10, 14, and 18 μM for IND. Insets are the variation of the anodic and peak currents versus concentration of each compound

in B-R buffer solution. So we used B-R buffer as electrolyte solution for all measurements. The effects of pH on electrochemical response of the MWCNT-IL/CCE toward the simultaneous determination of DCF and IND solutions were investigated. Dependences of peak current on the pH of the solution in the range of 5–12 are shown in Fig. 3a. It can be realized that the anodic peak currents of DCF and IND are increased slightly when there is an increase in the pH solution until it reaches 7.0. Thus pH 7.0 was selected as the optimum solution pH. As shown in Fig. 3b, all the anodic peak currents for the oxidation of DCF and IND shifted toward more negative potential with increasing pH value, which may be expressed by Eqs. 1 and 2, indicating that the protons have taken part in their electrode reaction processes.

$$\text{Diclofenac } E_p = -0.054\text{pH} + 1.0015 \quad R^2 = 0.9958 \quad (1)$$

$$\text{Indomethacin } E_p = -0.051\text{pH} + 0.9572 \quad R^2 = 0.9958 \quad (2)$$

Our results revealed that the numbers of protons in the processes are equal to the number of the transferred electrons. As shown in Scheme 2, DCF and IND can be oxidized via two electrons and two protons processes, respectively. This conclusion is in accordance with the known electrochemical reactions of DCF and IND as shown in other investigations [2, 29].

3.5 Effect of scan rate

To study the effect of potential sweep rate on the peak current, cyclic voltammetry was recorded at different

Table 1 Determination of IND in real samples ($n = 4$)

Sample	n	Content (mg)	Added (mg)	Founded (mg)	Recovery (%)	RSD (%)
Tablet	1	25	–	24.74	98.9	3.2
	2	25	5	30.48	101.6	3.1
	3	25	10	34.23	97.8	3.1
	4	25	15	39.73	99.4	3
Plasma	1	–	0.5	0.49	98	2.7
	2	–	2	2.02	101	2.9
	3	–	10	9.89	98.9	2.8
	4	–	15	14.68	97.9	2.7

Table 2 Determination of DCF in real samples ($n = 4$)

Sample	n	Content (mg)	Added (mg)	Founded (mg)	Recovery (%)	RSD (%)
Tablet	1	25	–	24	96	4.2
	2	25	5	29.1	97	4
	3	25	10	34.5	98.5	3.8
	4	25	15	39	97.5	3.9
Plasma	1	–	2	1.94	97	2.9
	2	–	5	4.88	97.6	2.8
	3	–	10	9.82	98.2	3.1
	4	–	25	24.9	99.6	3

Table 3 Analytical parameters for detection of DCF and IND at several methods

Drug type	Modified electrode	E_p (V)	L. R. (μM)	LOD (μM)	Ref.
DCF	Ni(OH) ₂ -nickel electrode	0.48	196–2,650	31.7	[30]
DCF	MWCNTs–surfactant GCE	0.69	0.17–2.5	0.08	[31]
DCF	Tyrosine-modified electrode	0.67	10–140	3.28	[32]
DCF	Cu-doped zeolite electrode	–	0.3–20	0.05	[33]
DCF	Edgeplane pyrolytic graphite	0.66	0.01–1	0.0062	[34]
IND	Ion-membrane electrode	–	100–50,000	30	[35]
IND	Ni(OH) ₂ -nickel electrode	0.55	5–79.4	1.41	[30]
IND	MWCNT–IL/CCE	0.77	1–50	0.26	This work
DCF	MWCNT–IL/CCE	0.55	0.05–50	0.018	This work

potential sweep rates in a wide range of 10–600 mV s^{-1} in B–R buffer solutions (pH 7.0) containing 0.5 mM DCF and 1.5 mM IND on the MWCNT–IL/CCE. The results showed that anodic peak current of IND varies linearly with the square root of the scan rate ($v^{1/2}$) and peak current of DCF versus scan rate was linear than its plot of peak current against $v^{1/2}$ (Fig. 4), confirming the diffusion-controlled process for electrooxidation of IND and surface-controlled process for DCF on the MWCNT–IL/CCE in the studied range of potential sweep rates regarding the following equations (Eqs. 3, 4):

$$\text{Diclofenac } I_p = 6.7718 v^{1/2} - 18.928 \quad R^2 = 0.965 \quad (3)$$

$$\text{Indomethacin } I_p = 0.0333 v^{1/2} - 0.0428 \quad R^2 = 0.998 \quad (4)$$

3.6 Simultaneous determination of DCF and IND

The electrooxidation processes of DCF and IND in the mixture were also investigated by DPV in B–R buffer solution (pH 7.0). When the concentration of one species changed, the other one was kept constant. Examination of Fig. 5 shows that the peak current of DCF increased with an increase in the DCF concentration while the concentration of IND was kept constant (2 μM). Similarly as can

be seen in Fig. 6, having kept the concentration of DCF constant ($2\text{ }\mu\text{M}$), the oxidation peak current of IND increases proportional to its concentration, while the oxidation peak current of DCF did not change. It should be noted that, the change of concentration of one compound did not have significant influence on the peak current and peak potential of the other compound. Moreover, when the concentrations of DCF and IND increased synchronously, the peak currents at the MWCNT–IL/CCE increase accordingly as shown in Fig. 7. It can be seen that the peak currents for the two species increased linearly with their concentrations (insets of Fig. 7). The calibration curves were linear for a wide range of concentrations of each species including $0.05\text{--}50\text{ }\mu\text{mol L}^{-1}$ DCF and $1\text{--}50\text{ }\mu\text{mol L}^{-1}$ IND. Detection limits of 18 and 260 nmol L^{-1} were observed for DCF and IND, respectively.

3.7 Determination of DCF and IND in real samples

The utilization of the proposed method in real sample analysis was also investigated by direct analysis of DCF and IND in commercial pharmaceutical and blood plasma samples by using DPV technique and results were listed in Tables 1 and 2. From these results, it can be seen that the WCNT–IL-modified CCE shows good catalytic activity for real sample analysis, especially in human plasma sample which has most of one hundred various biological and mineral compounds, and the obtained results and recoveries were satisfactory. Also, the results obtained for DCF and IND on a MWCNT–IL-modified CCE are compared in Table 3 with previously reported methods for their detections [29–34].

3.8 Reproducibility and long-term stability of the proposed electrode

The main advantage of using the MWCNT–IL/CCE is easy and quick surface renewal after each use. Thus, the repeatability of the analytical signal was studied by cyclic voltammetry in optimized conditions. The relative standard deviation (RSD) of 3 and 3.2 % for 1.0 mol L^{-1} DCF and 1.5 mol L^{-1} IND was obtained, respectively. Another attraction of the proposed modified electrode was that the resulting carbon paste electrode showed good long-term stability. Stability of the proposed electrode was tested by measuring the decrease in CV current of DCF and IND after being stored for 1 month. The CV response decreased by only 5 % indicating the suitable stability of MWCNTs–IL/CCE. The above results prove suitability of our fabricated electrode for practical applications.

4 Conclusions

We have shown that the MWCNT–IL composite-modified CCE exhibits high electrocatalytic activity to oxidation of DCF and IND. These drugs could be measured simultaneously at low levels by using the modified electrode with DPV method. Moreover, the results obtained from the application of the fabricated electrode for determination of DCF and IND in their tablets and plasma sample confirmed the good accuracy and precision of our fabricated electrode.

Acknowledgments The authors gratefully acknowledge the Research Council of Islamic Azad University, Ahar Branch, for financial support to carry out this research work.

References

- Kulling PEJ, Beckman Eva A, Skagius ASM (1995) Clin Toxicol 33:173
- Goyal RN, Chatterjee S, Rana ARS (2010) Carbon 48:4136
- Demertzi DK (2006) J Organomet Chem 691:1767
- Gostick N, James IG, Khong TK, Roy P, Shepherd PR et al (1990) Curr Med Res Opin 12:135
- Crowley B, Hamill JJ, Lyndon S, McKellican JF, Williams P et al (1990) Curr Med Res Opin 12:143
- Parrott RF, Vellucci SV (1998) Vasc Syst 30:65
- Radi A (1998) Electroanalysis 10:103
- Hirai T, Matsumoto S, Kishi I (1997) J Chromatogr B 692:375
- Reguera C, Ortiz MC, Arcos MJ (2002) Electroanalysis 14:1699
- Iijima S (1991) Nature 354:56
- Gaichore RR, Srivastava AK (2012) J Appl Electrochem 42:979
- Jain R, Sharma R (2012) J Appl Electrochem 42:341
- Sun L, Crooks RM (2000) J Am Chem Soc 122:12340
- Zhang L, Melechko AV, Merkulov VI, Guillorn MA, Simpson ML, Lowndes DH, Doktycz MJ (2002) Appl Phys Lett 81:135
- Saito Y, Tsujimoto Y, Koshio A, Kokai F (2007) Appl Phys Lett 90:213108
- Bonard JM, Weiss N, Kind H, Stocki T, Forro L, Kern K, Chatelain A (2001) Adv Mater 13:184
- Park C, Anderson PE, Chambers A, Tan CD, Hidalgo R, Rodriguez NM (1999) J Phys Chem B 103:10572
- Andraon JL, Armstrong DW, Wei GT (2006) Anal Chem 78:2892
- Buzzeo MC, Evans RG, Compton RG (2004) ChemPhysChem 5:1106
- Wang SF, Xiong HY, Zeng QX (2007) Electrochem Commun 9:807
- Kurachi A, Matsumiya M, Tsunashima K, Kodama S (2012) J Appl Electrochem 42:961
- DiCarlo CM, Compton DL, Evans KO, Laszlo JA (2006) Bioelectrochemistry 68:134
- Kubisa P (2004) Prog Polym Sci 29:3
- Heitzman H, Young BA, Rausch DJ, Rickert P, Stepinski DC et al (2006) Talanta 69:527
- Maleki N, Safavi A, Tajabadi F (2006) Anal Chem 78:3820
- Tsionsky M, Gun G, Glezer V, Lev O (1994) Anal Chem 66:1747
- Wu G, Xu BQ (2007) J Power Sour 174:148
- Henstridge MC, Laborda E, Dickinson EJJ, Compton RG (2012) J Electroanal Chem 664:73

29. Saghatforoush L, Hasanzadeh M, Karim-Nezhad G, Ershad S, Shadjou N et al (2009) Bull Korean Chem Soc 30:1341
30. Hajjizadeh M, Jabbari A, Heli H, Moosavi-Movahedi AA, Haghgoo S (2007) Electrochim Acta 53:1766
31. Yang X, Wang F, Hu S (2008) Mater Sci Eng C 28:188
32. Chethana BK, Basavanna S, Naik YA (2012) Ind Eng Chem Res 51:10287
33. Manea F, Ilios M, Remes A, Burtica G, Schoonman J (2010) Electroanalysis 22:2058
34. Goyal RN, Chatterjee S, Agrawal B (2010) Sens Actuators B 145:743
35. Kormosh Z, Hunka I, Bazel Y (2009) Mater Sci Eng C 29:1018